# Robust Adaptive Tracking Control for a Mechatronic Linear Drive System

Kun-Yung Chen, Assistant Professor
陳崑永
Department of Mechanical Engineering, Air Force Institute of Technology,
空軍航空技術學院一般學科部機械工程科

**Abstract**

In this paper, a mechatronic linear drive system is modeled and the adaptive controller is realized. In this system, unknown parameters are identified by particle swarm optimization, and adaptive tracking controller is designed to track the desired trajectory to overcome the nonlinear friction and external disturbance. Finally, it can be concluded that the the adaptive tracking controller can obtain the robustness performance for the mechatronic linear drive system. Numerical simulations demonstrate the adaptive tracking control strategy successfully.

**Key words:**Adaptive tracking control, Mechatronic linear drive system, Robust control.

## List of Symbols

| | | | |
|---|---|---|---|
| $c$ | damper coefficient | $c_{1\sim6}$ | constants |
| $f_c$ | coulomb frictional force | $f$ | control input force |
| $f_f$ | frictional force | $f_e$ | external force |
| $m_l$ | external loading mass | $f_s$ | static frictional force |
| $t_0$ | initial time | $m_0$ | mass of the slider table |
| $x$ | slider table's displacement | $t_f$ | final time |
| $\ddot{x}$ | slider table's acceleration | $\dot{x}$ | slider table's velocity |
| $\lambda_{1\sim2}$ | positive constants | $v_s$ | Stribeck velocity |
| $\varphi_{1\sim5}$ | positive constants | $\mu_k$ | coefficient of kinetic friction |
| $\sigma$ | positive constant | $\mu_s$ | coefficient of static friction |
| $B_m$ | motor damping coefficient | $J_m$ | motor moment of inertia |
| $K_t$ | motor torque constant | $K_v$ | positive constant |
| $L_d$ | screw lead | PMSM | permanent magnetic servo motor |

## 1 Introduction

The robust motion control with adaptive and sliding mode controller for mechatronic system was proposed in the previous studies [1-4]. The robustness of the controllers was emphasized. On the contrary, robust controller also consumes large input energy during the motion control process. Energy-saving motion control for the nonlinear mechatronic system is seldom considered but it is significant currently. It is naturally suggested that two advantages of the robustness and energy-saving motion control are necessarily considered simultaneously. In the previous researches [5-7], the authors proposed the minimum energy control theory to perform the minimum energy problems. But the definition of input energy was not the physical energy and the robustness performance was not considered. Kokotovic and Singh [8] presented the minimum-energy control for a second-order model of a ground transportation vehicle with a dc traction motor. The definition in performance index for minimum energy was a correct physical energy. However, their control approach cannot be employed in a nonlinear system.

The novelties and contributions of this paper are summarized as follows. (1) The mechanical disturbances including loading mass, viscous, coulomb frictional, static frictional and external forces are all considered for the mechatronic system. Therefore, a complete dynamic model of the mechatronic linear drive system is formulated. (2) A robust adaptive control is proposed to track the desired trajectory to demonstrate the robustness performance for the mechatronic system. Finally, numerical simulations successfully demonstrate that the adaptive tracking control has the robust and energy-saving performances.

## 2 Modeling

In the real application, all the parameters of the mechatronic linear drive system must be known firstly. The mechatronic linear drive system consists of the slider table driven by PMSM and is shown in Fig. 1. The dynamic formulation can be written as

$$f + f_f + f_e = (m_0 + m_l)\ddot{x}, \tag{1}$$

The block diagram of PMSM is described in Fig. 2. The PMSM torque can be transferred to the control input force by the screw, and the transfer equation can be written as follows:

$$\begin{aligned} f &= \frac{2\pi}{L_d}\tau = \frac{2\pi}{L_d}(K_t i_q - J_m \frac{2\pi}{L_d}\ddot{x} - B_m \frac{2\pi}{L_d}\dot{x}) \\ &= zK_t i_q - z^2 J_m \ddot{x} - z^2 B_m \dot{x}, \end{aligned} \tag{2}$$

where $z = 2\pi / L_d$. Substituting Eq. (2) into Eq. (1), it can be obtained the following equation

$$(m_0 + m_l + z^2 J_m)\ddot{x} + z^2 B_m \dot{x} = zK_t i_q + f_f + f_e. \tag{3}$$

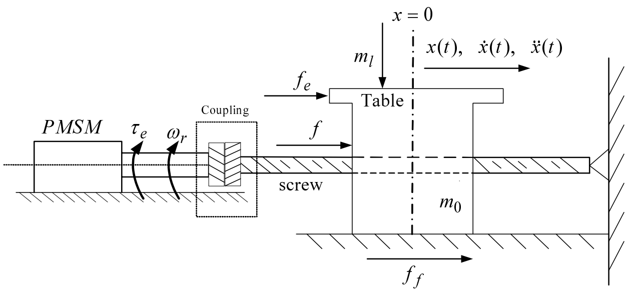


Fig. 1 Physical model of the mechatronic linear drive system.

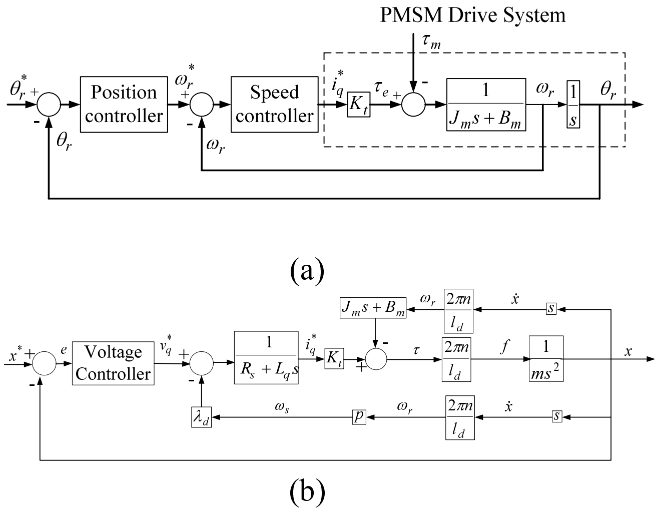


Fig. 2 Block diagrams of the PMSM drive system: (a) control system; (b) voltage controller.

In Eq. (3), the frictional force $f_f$ in LuGre frictional model is employed as follows:

$$f_f = -f_c \operatorname{sgn}(\dot{x}) - (f_s - f_c)\exp(-(\frac{\dot{x}}{v_s})^2)\operatorname{sgn}(\dot{x}) - c\dot{x}, \tag{4}$$

where $f_c = (m_0 + m_l)g\mu_k$ and $f_s = (m_0 + m_l)g\mu_s$. Therefore, the dynamic equation of the linear drive system with frictional and control input forces can be found as follows:

$$\begin{aligned} &(m_0 + m_l + z^2 J_m)\ddot{x} + (c + z^2 B_m)\dot{x} \\ &= zK_t i_q - (m_0 + m_l)g\operatorname{sgn}(\dot{x})[\mu_k + (\mu_s - \mu_k)\exp(-(\frac{\dot{x}}{v_s})^2)] + f_e. \end{aligned} \tag{5}$$

In the industrial application of a PMSM, the voltage command is used as the control input voltage [9], which can be described as follows:

$$v_q = R_s i_q + L_q \frac{d}{dt} i_q + \lambda_d \omega_r = R_s i_q + L_q \frac{d}{dt} i_q + \lambda_d z\dot{x}. \tag{6}$$

Finally, Eqs (5) and (6) are combined as a matrix form as follows:

$$\dot{\mathbf{X}} = \mathbf{A}\mathbf{X} + \mathbf{B}u + \mathbf{D}, \tag{7}$$

where $\mathbf{X} = [x_1 \quad x_2 \quad x_3]^T$, $x_1 = x$, $x_2 = \dot{x}$, $x_3 = i_q$, $\mathbf{A} = \begin{bmatrix} 0 & 1 & 0 \\ 0 & -N/M & Q/M \\ 0 & -\lambda_d z / L_q & -R_s / L_q \end{bmatrix}$,

$\mathbf{B} = [\,0 \quad 0 \quad 1/L_q\,]^T$,

$\mathbf{D} = [\,0 \quad d/M \quad 0\,]^T$, $M = m_0 + m_l + z^2 J_m$,

$N = c + z^2 B_m$, $Q = zK_t$, $u = v_q$,

$$d = -(m_0 + m_l)g\operatorname{sgn}(x_2)[\mu_k + (\mu_s - \mu_k)\exp\left(-(\frac{x_2}{v_s})^2\right)] + f_e.$$

## 3 Design of adaptive tracking controller

In order to design an adaptive controller, Eq. (5) can be rewritten as follows:

$$\dot{x}_2 = \frac{-(c+z^2B_m)}{(m+z^2J_m)}x_2 + \frac{zK_t}{(m+z^2J_m)}x_3 - \frac{f_c\,\mathrm{sgn}(x_2)}{(m+z^2J_m)}[1-\exp\left(-(\frac{x_2}{v_s})^2\right)] - \frac{f_s\,\mathrm{sgn}(x_2)}{(m+z^2J_m)}\exp\left(-(\frac{x_2}{v_s})^2\right) + \frac{f_e}{(m+z^2J_m)}, \quad (8)$$

It is assumed that $c$, $f_c$, $f_s$ and $f_e$ are not exactly known. With these uncertainties, the first step in designing an adaptive controller is to select a Lyapunov function, which is a function of tracking error and the parameters' errors. An inertia-related Lyapunov function containing a quadratic form of a linear combination of the errors of displacement, speed and current is chosen as follows [10]:

$$V = \frac{1}{2}L_q s_e + \frac{1}{2}\tilde{\boldsymbol{\varphi}}^{\mathbf{T}}\boldsymbol{\Phi}^{-\mathbf{1}}\tilde{\boldsymbol{\varphi}}, \quad (9)$$

where $\boldsymbol{\Phi} = diag(\phi_1,\ \phi_2,\ \phi_3,\ \phi_4,\ \phi_5)$, $s_e = \boldsymbol{\Lambda}\mathbf{E}$, $\boldsymbol{\Lambda} = [\lambda_1 \quad \lambda_2 \quad 1]$, $\mathbf{E} = [e_1 \quad e_2 \quad e_3]^T$, $e_1 = x_1^* - x_1$, $e_2 = x_2^* - x_2$, $e_3 = x_3^* - x_3$,

$\tilde{\boldsymbol{\varphi}} = \boldsymbol{\varphi} - \hat{\boldsymbol{\varphi}} = \left[\, m-\hat{m} \quad c-\hat{c} \quad f_c-\hat{f}_c \quad f_s-\hat{f}_s \quad f_e-\hat{f}_e \,\right]^T$,

$\boldsymbol{\varphi} = [m \quad c \quad f_c \quad f_s \quad f_e]^T$, $\hat{\boldsymbol{\varphi}} = [\hat{m} \quad \hat{c} \quad \hat{f}_c \quad \hat{f}_s \quad \hat{f}_e]^T$,

and $\hat{\boldsymbol{\varphi}}$ is the estimated vector of parameters. The auxiliary signal $s_e$ can be considered as a filtered tracking error. Differentiating Eq. (9) with respect to time, it is found as

$$\dot{V} = s_e L_q \dot{s}_e + \tilde{\boldsymbol{\varphi}}^{\mathbf{T}}\boldsymbol{\Phi}^{-\mathbf{1}}\dot{\tilde{\boldsymbol{\varphi}}}. \quad (10)$$

The item $L_q\dot{s}_e$ in Eq. (10) can be written as follows:

$$\begin{aligned} L_q\dot{s}_e &= L_q[\lambda_1(\dot{x}_1^* - \dot{x}_1) + \lambda_2(\dot{x}_2^* - \dot{x}_2) + (\dot{x}_3^* - \dot{x}_3)] \\ &= L_q[\lambda_1(x_2^* - x_2) + \lambda_2(\dot{x}_2^* - \dot{x}_2) + \dot{x}_3^*] - u + \lambda_d z x_2 + R_s x_3. \end{aligned} \quad (11)$$

$x_3$ in Eq. (5) can be arranged and written as follows:

$$x_3 = \frac{\dot{x}_2}{zK_t}m + \frac{x_2}{zK_t}c + \frac{\mathrm{sgn}(x_2)}{zK_t}[1-\exp\left(-(\frac{x_2}{v_s})^2\right)]f_c + \frac{\mathrm{sgn}(x_2)}{zK_t}\exp\left(-(\frac{x_2}{v_s})^2\right)f_s - \frac{1}{zK_t}f_e + \frac{z^2J_m}{zK_t}\dot{x}_2 + \frac{z^2B_m}{zK_t}x_2. \quad (12)$$

Substituting Eq. (12) into Eq. (11), it can be found as follows:

$$\begin{aligned} L_q\dot{s}_e &= L_q[\lambda_1(x_2^* - x_2) + \lambda_2(\dot{x}_2^* - \dot{x}_2) + \dot{x}_3^*] - u + \lambda_d z x_2 \\ &+ \frac{R_s\dot{x}_2}{zK_t}m + R_s\frac{x_2}{zK_t}c + \frac{R_s\,\mathrm{sgn}(x_2)}{zK_t}[1-\exp\left(-(\frac{x_2}{v_s})^2\right)]f_c \\ &+ \frac{R_s\,\mathrm{sgn}(x_2)}{zK_t}\exp\left(-(\frac{x_2}{v_s})^2\right)f_s - \frac{R_s}{zK_t}f_e + \frac{R_s z^2 J_m}{zK_t}\dot{x}_2 + \frac{R_s z^2 B_m}{zK_t}x_2 \\ &= \mathbf{Z}(\bullet)\boldsymbol{\varphi} + Y(\bullet) - u. \end{aligned} \quad (13)$$

where

$$Z(\bullet) = \left[ \frac{R_s\dot{x}_2}{zK_t} \quad \frac{R_s x_2}{zK_t} \quad \frac{R_s\,\mathrm{sgn}(x_2)}{zK_t}[1-\exp\left(-(\frac{x_2}{v_s})^2\right)] \quad \cdots \quad \frac{R_s\,\mathrm{sgn}(x_2)}{zK_t}\exp\left(-(\frac{x_2}{v_s})^2\right) \quad -\frac{R_s}{zK_t} \right], \quad (14\text{-}1)$$

$$Y(\bullet) = L_q[\lambda_1(x_2^* - x_2) + \lambda_2(\dot{x}_2^* - \dot{x}_2) + \dot{x}_3^*] + \frac{R_s z^2 J_m}{zK_t}\dot{x}_2 + (\lambda_d z + \frac{R_s z^2 B_m}{zK_t})x_2. \quad (14\text{-}2)$$

Therefore, Eq. (10) can be rewritten as follows:

$$\dot{V} = s_e L_q \dot{s}_e + \tilde{\boldsymbol{\varphi}}^{\mathbf{T}}\boldsymbol{\Phi}^{-\mathbf{1}}\dot{\tilde{\boldsymbol{\varphi}}} = s[\mathbf{Z}(\bullet)\boldsymbol{\varphi} + Y(\bullet) - u] + \tilde{\boldsymbol{\varphi}}^{\mathbf{T}}\boldsymbol{\Phi}^{-\mathbf{1}}\dot{\tilde{\boldsymbol{\varphi}}}. \quad (15)$$

It can let the adaptive control law $u$ be

$$u = \mathbf{Z}(\bullet)\hat{\boldsymbol{\varphi}} + Y(\bullet) + K_v s_e, \quad (16)$$

Then, Eq. (15) becomes as

$$\dot{V} = -K_v s_e^2 + \tilde{\boldsymbol{\varphi}}^T[\mathbf{Z}^T(\bullet)s_e + \boldsymbol{\Phi}^{-\mathbf{1}}\dot{\tilde{\boldsymbol{\varphi}}}]. \quad (17)$$

Let

$$\mathbf{Z}^T(\bullet)s_e + \boldsymbol{\Phi}^{-\mathbf{1}}\dot{\tilde{\boldsymbol{\varphi}}} = 0, \quad (18)$$

and select the adaptive update rule as

$$\dot{\hat{\boldsymbol{\varphi}}} = \boldsymbol{\Phi}\mathbf{Z}^{\mathrm{T}}(\bullet)s_e. \quad (19)$$

Then Eq. (17) becomes

$$\dot{V} = -K_v s_e^2 \le 0. \quad (20)$$

As $\dot{V}$ is negative semi-definite, then $V$ is upper-bounded. As $V$ is upper-bounded, it can be said that $s_e$ and $\tilde{\varphi}$ are bounded. From the definition of $s_e$ given in Eq. (9), then $e_1$, $e_2$ and $e_3$ are bounded. As $e_1$ , $e_2$ , $e_3$ , $s_e$ and $\tilde{\varphi}$ are bounded, it can be shown that $\dot{s}_e$ is bounded and hence $\ddot{V}$ is also bounded. From the above description, Barbalat's Lemma can be used to state that $\lim_{t\to\infty}\dot{V}=0$. By using Rayleigh-Ritz theorem for $\dot{V}$ , then $\lim_{t\to\infty}s_e=0$. From $s_e=\mathbf{\Lambda E}$, it can be stated that $\lim_{t\to\infty}e_1=0$, $\lim_{t\to\infty}e_2=0$ and $\lim_{t\to\infty}e_3=0$. It is concluded that the tracking errors $e_1$, $e_2$ and $e_3$ are asymptotically stable. On the other hand, the guaranteed convergence of the tracking errors to zero does not imply the convergence of the

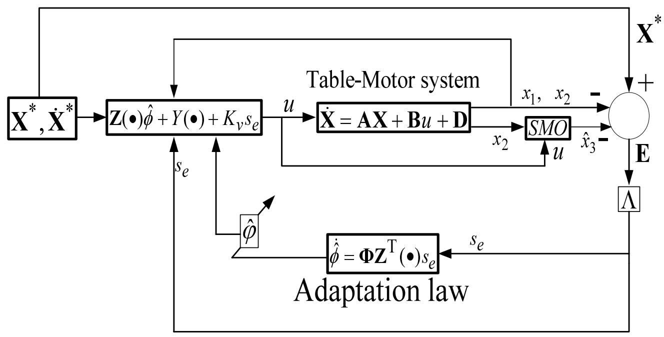


Fig. 3 Adaptive tracking control block diagram.

estimated parameters to the exact values. Finally, the proposed adaptive tracking control block diagram for the mechatronic linear drive system is shown in Fig. 3.

## 4 Numerical simulation

In numerical simulations, the numerical parameters' values are given as follows:

$m=0.5$ kg, $c=0.5$ Ns/m $\mu_k=0.1$, $\mu_s=0.2$, $v_s=10^{-3}$ m/s, $K_t=0.8$ Nm/A, $J_m=8\times10^{-4}$ Nms$^2$, $B_m=2\times10^{-2}$ Nms/rad, $L_d=0.01$ m, $R_s=0.2$ Ω, $L_q=10^{-3}$ H, $\lambda_d=10^{-3}$ HA.

In order to perform the robust performance of the proposed adaptive tracking controller, it is assumed the uncertainties are $m_l=2$ kg , $c=1$ Ns/m and $f_e=10\cos 2\pi t$ $N$. The other disturbances including coulomb frictional force and static frictional force are also applied to the system. The desired trajectories are given as $x_1^*(t)=\sin 2\pi t$ $m$, $x_2^*(t)=2\pi\cos 2\pi t$ $m/s$ and $x_3^*(t)=[M_0\dot{x}_2(t)+Nx_2(t)]/Q$ $A$, and the initial conditions are $x_1(0)=0.5$ $m$, $x_2(0)=0$ $m/s$, and $x_3(0)=0$ $A$. By substituting the above parameters into Eq. (7), the system becomes an initial-value problem and can be integrated by using the fourth-order Runge-Kutta method with time step $\Delta t=0.001$ s, and tolerance error $10^{-9}$. The robust performance of the proposed adaptive tracking controller can be seen in Fig. 4. It is found from Figs. 4(a)-(f) that the output responses rapidly converge toward desired trajectories after 0.5 s. The adaptive control input $u$ demonstrates the robustness to overcome the external force in Fig. 4(g). The steady-state error $s_e$ converges to a small range $s_e=0$, which is shown in Fig. 4(h). The results can demonstrate the robust performance in the proposed adaptive control.

## 5 Conclusion

Robustness control for the mechatronic linear drive system are performed by adaptive tracking control in this paper. The complete model is formulated to have the voltage control input for this system. Finally, the robust adaptive control is employed to track the designed trajectory under the disturbances and

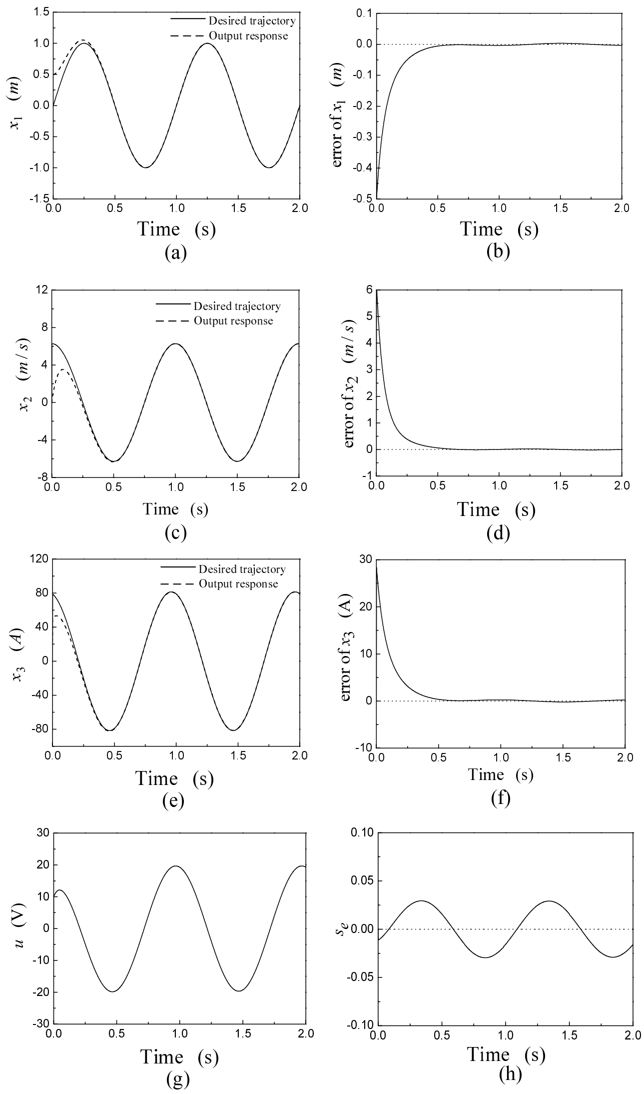


Fig. 4 Numerical tracking performance of the proposed adaptive controller.

frictional forces. Numerical tracking results demonstrate that the adaptive controller can obtain the robust control for the mechatronic linear drive system.

## References

[1] F. J. Lin, R. F. Fung and Y. S. Lin, “Adaptive control of slider-crank mechanism motion: simulations and experiments,” *Int. J. Syst.*, vol. 28, no. 12, pp. 1227-1238, Jun. 1997.

[2] C. W. Chuang, M. S. Huang, K. Y. Chen and R. F. Fung, “Adaptive vision-based control of a motor-toggle mechanism: Simulations and experiments,” *J. Sound Vibr.,* vol. 312, pp. 848–861, May. 2008.

[3] F. J. Lin, R. F. Fung and Y. C. Wang,” Sliding mode fuzzy control of toggle mechanism using PM synchronous servomotor drive,” *IEE Proc-Control theory Appl*. vol. 144, no. 5, pp. 393-402, Sep. 1997.

[4] R. F. Fung, F. J. Lin, J. S. Huang and Y. C. Wang,” Application of sliding mode control with a low pass filter to the constantly rotating slider-crack mechanism,” *JSME Int. J. Series c*, vol. 40, no. 4, pp. 717-722, Dec. 1997.

[5] T. Kaczorek, “Reachability and minimum energy control of positive 2D systems with delays,” *Control and Cybernetics,* vol. 34, no. 2, Jul. 2005.

[6] C. Botan, V. Horga, F. Ostafi, M. Ratoi, “Minimum energy and minimum time control of electrical drive systems,” *WSEAS Trans. Power Syst*., vol. 3, no. 4, pp. 141-150, Apr. 2008.

[7] T. Kaczorek, “Minimum energy control of positive continuous-time linear systems with bounded inputs,” *Int. J. Appl. Math. Compu.. Sci*, vol. 23, no. 4, pp. 725-730, Aug. 2013.

[8] P. Kokotovic and G. Singh, “Minimum-energy control of a traction motor,” *IEEE Trans. Autom. Control,* short papers, pp. 92-95, 1972.

[9] K. Y Chen, M. S Huang, and R. F Fung, “Adaptive minimum-energy tracking control for the mechatronic elevator system,” *IEEE Trans. Control Syst. Technol.,* In Press, 2014. ( http://ieeexplore.ieee.org.)

[10] K. Y Chen, M. S Huang, and R. F. Fung, "Adaptive tracking control for a motor-table system." *IEEE/ASME Int. Conf on Advanced Intelligent Mechatronics*, Kaohsiung, Taiwan, pp. 1054-1059, Jul. 2012.